CRACK PROPAGATION AND ARREST IN PRESSURIZED CONTAINERS

by

F. Erdogan
F. Delale
J. A. Owczarek

Lehigh University
Bethlehem, Pennsylvania

March 1976

THE NATIONAL AERONAUTICS AND SPACE ADMINISTRATION GRANT NGR39-007-011

CRACK PROPAGATION AND ARREST IN PRESSURIZED CONTAINERS

by

F. Erdogan
F. Delale
J. A. Owczarek

Lehigh University
Bethlehem, Pennsylvania
March 1976

THE NATIONAL AERONAUTICS AND SPACE ADMINISTRATION GRANT NGR39-007-011

LIST OF SYMBOLS

$a(t)$	=	half crack length at time t
$2a_o$	=	initial crack length
b_i, c_i	=	crack propagation constants
C_D	=	discharge coefficient
$D(t)$	=	crack opening or orifice area
E	=	modulus of elasticity
h:	=	wall thickness of the cylinder
$k(t)$	=	stress intensity factor
k_c	=	critical stress intensity factor
ℓ	=	length of the cylinder
m_o	=	initial mass of the gas
$p(t)$	=	gas pressure inside the cylinder
p_o	=	initial gas pressure
$p_R(t)$	=	resistance pressure or load carrying capacity
R	=	gas constant
R_o	=	mean radius of curvature of the cylinder
$T(t)$	=	absolute gas temperature
T_o	=	initial gas temperature
t	=	time
V	=	volume of the container
$v(t)$	=	crack velocity
γ	=	ratio of specific heats
$\lambda(t)$	=	shell parameter
$\rho(t)$	=	gas density

CRACK PROPAGATION AND ARREST IN PRESSURIZED CONTAINERS(*)

by

F. Erdogan, F. Delale, and J. A. Owczarek
Lehigh University, Bethlehem, Pennsylvania

Abstract. The problem of crack propagation and arrest in a finite volume cylindrical container filled with pressurized gas is considered. It is assumed that the cylinder contains a symmetrically located longitudinal part-through crack with a relatively small net ligament. The net ligament suddenly ruptures initiating the process of fracture propagation and depressurization in the cylinder. Thus the problem is a coupled gas dynamics and solid mechanics problem the exact formulation of which does not seem to be possible. It is formulated by making two major assumptions, namely that the shell problem is quasi-static and the gas dynamics problem is one-dimensional. The problem is reduced to a proper initial value problem by introducing a dynamic fracture criterion which relates the crack acceleration to the difference between a load factor and the corresponding strength parameter. The main results are demonstrated by considering two examples, an aluminum cylinder which may behave in a quasi-brittle manner, and a steel cylinder which undergoes ductile fracture. The results indicate that generally in gas-filled cylinders fracture arrest is not possible unless the material behaves in a ductile manner and the container is relatively long.

(*) This work was supported by the Materials Division, NASA-Langley under the Grant NGR 39-007-011 and by NSF under the Grant ENG 73-045053 A01.

1. INTRODUCTION

In studying the fracture failure of relatively thin-walled pressure vessels and pipes, in general one may consider the phenomenon in three different phases. The first is the subcritical crack propagation starting from a localized imperfection. This initial flaw which may form the nucleus of a dominant crack in the cylinder wall may be a material or manufacturing defect, or may be accidentally induced. Even though such flaws are just as likely to be fully imbedded interior defects, from the viewpoint of subcritical crack growth, it is the surface flaw which is of more critical concern. The reason for this is the presence of higher level stresses near and at the surfaces and the likelihood of ready exposure to adverse environmental conditions. Once the crack is nucleated, the subcritical crack propagation may be due to low cycle fatigue and stress corrosion cracking.

In the heavy-section low toughness structures if the subcritically growing crack reaches a "critical" size, it is possible to have a plane strain type of fracture leading to catastrophic failure. However, in most cases, particularly in relatively thin-walled cylinders, there is sufficient amount of plastic deformation around the leading edge of the part-through crack so that before the crack reaches the critical size the net ligament between the crack front and the opposing surface would be fully yielded (Figure 1). In such cases, the second phase of the failure process would then be (generally ductile) fracture of the net ligament. The net ligament rupture may occur as a result of progressive stable crack growth. However, for materials with relatively high fracture toughness, perhaps a more likely rupture mechanism is the "net ligament plastic instability" described in [1].

Even though in some cases it is theoretically possible to have "leak" before "burst", in practical situations it turns out that in both brittle as well as ductile type of fracture, the internal pressure which is high enough to cause the net ligament to rupture is usually above the critical level which can be sustained by a cylinder with a through crack having the same length $2a_o$ as the part-through crack [1] (Figure 1). Thus, the

final phase of the fracture failure in pressurized cylinders is the propagation of a through crack. This is clearly a coupled fracture dynamics and fluid mechanics or gas dynamics problem. Whether the fracture propagation would result in catastrophic failure or crack arrest would, of course, depend on the nature of decompression in the cylinder as the liquid or gas is discharged through the orifice provided by the propagating crack.

From the structural view point the tools dealing with the subcritical crack growth phenomenon appear to be fairly well-understood and quite adequate [2,3]. If the particular part-through crack problem can be solved (see, for example [4,5]), then the crack propagation rate under fatigue or stress corrosion cracking may be estimated by using certain empirically established models [2,3,6,7]. A quantitative modeling of fully-yielded net ligament in shells is somewhat more complicated. However, in this case too adequate results may be obtained by properly considering the plasticity effects [1,8,9]. On the other hand, it would be no exaggeration to state that the crack propagation phase of the fracture failure following the net ligament rupture is not understood at all. In this paper, after making some remarks regarding the fracture dynamics in relatively thin-walled pressurized containers mostly for the purpose of pointing out the extremely complex nature of the problem, the quasi static fracture propagation problem for the finite volume containers is considered. Two types of fracture models applicable to materials with essentially brittle or ductile fracture behavior are developed and some numerical examples are given.

2. ON THE FRACTURE DYNAMICS IN PRESSURIZED CONTAINERS

Consider a relatively thin-walled pressurized cylindrical container of finite volume. Let a symmetrically located meridional through crack of length $2a_o$ suddenly appear in its wall as a result of net ligament rupture (Figure 1). The ensuing phenomenon may be considered as an initial value problem with, for example, the components of the displacement vector u_1, u_2, and u_3 in the cylinder wall and the components of the velocity vector v_1, v_2, and v_3, the pressure p, the temperature T, and the density ρ

of the liquid or gas inside the cylinder as the basic state variables which are functions of time and space coordinates. Considering the symmetry of the problem and assuming that no crack branching takes place, the problem has at least one more unknown function which is the crack length a(t). The crack surface displacements which determine the size and the shape of the "orifice" are given by the displacement components u_1, u_2, and u_3. By using the basic physical principles, theoretically it should be possible to write nine field equations (e.g., equations of state and energy, and conservation of mass and momentum), to account for the nine basic unknown functions u_i, v_i, (i=1,2,3), p, T, and ρ. These equations may be expressed in terms of a system of differential operators as follows:

$$L_i(u_j, v_j, p, \rho, T) = 0, \quad (i=1,..,9, \ j=1,2,3) \ . \tag{1}$$

Equations (1) will be subject to standard initial conditions, the conditions of continuity on the inner surface of the cylinder regarding the traction and the velocity components, and the traction boundary conditions on the outer surface of the cylinder and on the surface of the crack. Even if there is no crack propagation after the rupture of net ligament, the general dynamic problem is intractable. The reason for this is that in considering the gas dynamics or the fluid mechanics, it does not seem to be possible to express the boundary conditions at the opening on the cylinder wall created by the crack in an exact manner.

If the crack continues to propagate after the rupture of net ligament, the problem is further complicated by the fact that it now has a moving boundary. In this case, technically one may complete the formulation of the problem by considering an additional unknown function which represents the crack size, such as the half crack length a(t), and an additional condition, such as a fracture criterion of the form

$$F(u_i, p, a, c_j) \geq 0 \tag{2}$$

which states that a certain minimum condition must be met for propagation of the crack. In (2) the displacements u_i, (i=1,2,3) represent the stress or the strain field in the cylinder, the nonuniform pressure p represents

the applied load which may appear in the criterion explicitly as well as through u_i, and c_j (j=1,2,..) are the constants representing the yield and fracture resistance behavior of the material. Ordinarily, in structural mechanics the form of the fracture criterion as given by (2) and, for example, expressed in terms of the stress intensity factor $k \geq k_{IC}$, the strain energy release rate $G \geq G_{IC}$, the J-integral, or the K_R-curve is adequate if one is only interested in the question of stability of the crack under a given set of loading conditions which are usually either fixed load or fixed displacement type. However, it is clear that in a coupled problem of fracture dynamics-fluid mechanics, it is not sufficient to say that the fracture will take place if certain minimum conditions are met and exceeded. It is at the same time necessary to make some specific statements regarding the dependence of the fracture acceleration and deceleration or fracture velocity on the load level. More specifically, the fracture criterion must express the dependence of some time rate of change of the fracture area on the difference between a load factor representing the intensity of the applied load and a corresponding strength parameter which represents the fracture resistance of the material. Lack of phenomenological understanding and adequate modeling has been one of the major difficulties in studying the problem of fracture dynamics in structural solids. Because of this in most of the existing studies rather than considering a physically acceptable fracture criterion, an inverse technique is adopted by specifying the crack velocity [5,10].

3. A QUASI STATIC MODEL FOR GAS-FILLED CYLINDERS

Consider now a cylindrical shell of length ℓ, mean radius of curvature R_o, and thickness h. Initially let the cylinder be filled with gas of pressure p_o and (absolute) temperature T_o. It is assumed that the cylinder contains a symmetrically located part-through longitudinal crack with a relatively small net ligament thickness (Figure 1). At time t=0 the net ligament ruptures creating a through crack of length $2a_o$. Let the pressure p_o be greater than the value which can be sustained by a cylindrical shell having a through crack of length $2a_o$. Thus, the crack will start growing upon the rupture of net ligament and, because of the gas outflow through the crack opening, the container will start to depressurize. From the

view point of crack propagation, similar to flat plates, under constant load the cracked cylindrical shell is basically unstable. However, because of depressurization there is a possibility of crack arrest before catastrophic failure. It is therefore clear that the problem of fracture dynamics is strongly coupled with the problem of gas dynamics.

To develop any type of an acceptable analytical model for the problem two major obstacles need to be overcome. As pointed out earlier, the exact formulation of the related gas dynamics problem does not seem to be possible. Therefore, even if the necessary mathematical techniques to solve such problems were to be available, without any approximating assumptions the problem would be intractable. This then is the first major aspect of the phenomenon which requires certain physically acceptable simplifying assumptions so that an analytical treatment of the problem is possible. The second major aspect of the phenomenon refers to fracture dynamics which is fundamentally much less understood. In the present coupled problem to use the so-called inverse method which assumes the velocity or the acceleration of the crack beforehand would be meaningless. The key question in this respect is this: in what way is the crack propagation behavior (say, its velocity or acceleration) dependent on the load factor which represents the intensity of the applied load and the geometry? Without making some statement to this effect, clearly the crack propagation and arrest problem cannot be treated as a dynamic phenomenon.

Consider now the first aspect of the phenomenon, namely the formulation of the coupled solid mechanics-gas dynamics problem. To render the problem tractable and bring it down to manageable proportions, in this study the following approximating assumptions will be made:

(a) In the shell analysis the inertia effects will be neglected and the problem will be treated as being quasi-static. Even though there are no available solutions to the dynamic shell problem, using the flat plate results as guide it may be stated that the inertia effects will be negligible provided the crack velocity remains below approximately one-fourth of the shear wave velocity of the shell material [10]. As will be seen from numerical examples, in the finite volume containers this ceiling for the

crack velocity and hence, the quasi-static assumption does not seem to be very unrealistic.

(b) The compressed gas in the container behaves like an ideal gas with constant specific heats.

(c) The pressure drop in the container is sufficiently slow so that the gas dynamics problem may be treated as being "one-dimensional" with the (space-independent) basic variables pressure p, temperature T, and density ρ.

(d) The discharge through the crack opening is at sonic velocity with a constant discharge coefficient C_D, i.e., it is assumed that

$$\frac{p_e}{p(t)} \leq \left(\frac{2}{1+\gamma}\right)^{\frac{\gamma}{\gamma-1}} \tag{3}$$

where p is the gas pressure in the containers, p_e is the environmental pressure, $\gamma = c_p/c_v$, c_p and c_v being the specific heats under constant pressure and constant volume, respectively.

(e) The crack opening or the "orifice" may be approximated by an ellipse with the crack length and the crack opening displacement in the center of the crack as the major axes. Using the results given in [11] and extrapolating them the crack opening area may be approximated by

$$D(t) = \pi a^2 p \left[\frac{2R_o}{hE} + \frac{1.47a^2}{h^2E}\right] \tag{4}$$

where E is the elastic modulus of the cylinder.

Under these assumptions it is seen that the unknown functions are p, ρ, T, and a with t as the independent variable. The conditions to determine these functions are

(i) the equation of state for the gas

$$\frac{p}{\rho} = RT \tag{5}$$

where R is the gas constant;

(ii) the isentropic process equation

$$p\rho^{-\gamma} = \text{constant}; \tag{6}$$

(iii) the conservation of mass which states that the rate of mass outflow through the orifice is the same as the rate of mass reduction in the container and which may be expressed as

$$\frac{d}{dt}(m_o - V\rho) = C_D D \rho_* u_* \ , \tag{7}$$

where m_o is the initial mass of the gas, V is the container volume, C_D is the discharge coefficient, and D is the crack or orifice area. The quantities ρ_* and u_* are, respectively, the gas density and velocity at the smallest exit section where sonic flow conditions are assumed to prevail, and are given by

$$\rho_* = \rho\left(\frac{2}{1+\gamma}\right)^{\frac{1}{\gamma-1}} \ , \quad u_* = \left(\frac{2}{1+\gamma} RT\right)^{\frac{1}{2}} \ . \tag{8}$$

Eliminating ρ and T, from equations (4) to (8) it follows that

$$\frac{dp}{dt} = -\frac{\pi C_D}{V}\left(\frac{2}{\gamma+1}\right)^{\frac{\gamma+1}{2(\gamma-1)}} \frac{\gamma\sqrt{\gamma RT_o}}{p_o^{(\gamma-1)/2\gamma}}\left(\frac{2R_o}{hE} + \frac{1.47a^2}{h^2E}\right)a^2 p^{(5\gamma-1)/2\gamma} \tag{9}$$

where T_o and p_o are the initial gas temperature and pressure in the container.

(iv) Dynamic fracture criterion. A fracture criterion stated in the form of an inequality such as (2) can only refer to fracture initiation or to a static condition. In order to treat dynamic crack propagation problems, the criterion must also be dynamic in nature and must properly relate "the crack driving force" to the crack length and its time derivatives. In expressing the dynamic fracture criteria used in this study, two basic physical assumptions are made which are intuitively motivated. It is assumed that first the crack acceleration or velocity is a function of the "crack driving force" and secondly, if the crack driving force is negative, in structural metallic materials there is a fracture deceleration phase and the deceleration rate is much higher than the crack acceleration rate. The next step is the proper selection of the "crack driving force" which will be dependent on the fracture behavior of the material. In brittle or quasi-brittle type materials it is realistic to assume that(*) $k-k_c$ or $G-G_c$ is

(*) Here the critical values k_c and G_c may be velocity dependent and may not be the same as the plane strain values K_{IC} and G_{IC}. In this sense, the model has some flexibility and may accommodate the phase of the fracture which may not be completely plane strain in nature.

the crack driving force where k is the time-dependent stress intensity factor at the crack tip, k_c is a critical value which has to be exceeded for fracture initiation and growth, G and G_c are the strain energy release rate and fracture toughness and are related to k^2, k_c^2, respectively.

The experiments on glass plates indicate that "the crack has no inertia". The meaning of this statement and the related conclusions are that the crack velocity is always in phase with the crack driving force, the velocity is a function of the crack driving force alone, and crack branching occurs when the input energy (or the crack driving force) becomes too high to be dissipated by a single crack and takes place at a certain limiting crack velocity (approximately half the shear wave velocity). Since the limiting crack velocity implies increased fracture resistance at higher crack velocities, for ideally brittle materials the dynamic fracture criterion may be expressed by relating the crack velocity to $k-k_c$ or $G-G_c$. Assuming that $G \sim k^2$, one may, for example, write

$$\frac{da}{dt} = \begin{cases} \sum_{1}^{N} d_n (k^2-k_c^2)^n, & \text{for } k > k_c \\ 0, & \text{for } k < k_c \end{cases} \tag{10}$$

where $d_1,..,d_N$ are constant, k is generally a function of a, and k_c is a function of da/dt. In the range of crack velocities for which the inertia effects are negligible, k_c may be assumed constant and the differential equation (10) with (9) would determine the functions a(t) and p(t).

Intuitively it could be argued that in metallic materials with varying degrees of plastic behavior the instantaneous change in velocity implied by (10) is not possible and the phenomenon must exhibit some inertia. In this case the dynamic fracture criterion must include crack acceleration as well as the velocity. Also, if the plasticity effects are not appreciable, k or G may be used as the crack driving force and the fracture criterion in its simplest form may be expressed as

Model I:

$$\frac{d^2a}{dt^2} = \begin{cases} b_1(k-k_c), & \text{for } k > k_c, \\ b_1(k-k_c) - b_2(k-k_c)^2, & \text{for } k < k_c, \end{cases} \tag{11}$$

or Model II:

$$\frac{d^2a}{dt^2} = \begin{cases} b_3(k^2-k_c^2) \ , \ \text{for } k > k_c \ , \\ b_3(k^2-k_c^2) - b_4(k^2-k_c^2)^2 \ , \ \text{for } k < k_c \end{cases} \tag{12}$$

where $b_1,\ldots,b_4$ are constant.

The stress intensity factor k is obtained from the elastic solution of the shell problem (e.g., [12,13]). Extrapolated for large values of the shell parameter λ, the stress intensity factor for the pressurized cylindrical shell with an axial crack may be approximated by

$$k = \frac{pR_o}{h} \sqrt{\pi a}\, A(\lambda) \ , \tag{13}$$

$$A(\lambda) = \begin{cases} 0.5\lambda + 0.6 + 0.4e^{-1.25\lambda} \ , \ \text{for } \lambda \leq 5 \\ 1.761\sqrt{\lambda-1.9} \ , \ \text{for } \lambda > 5 \ , \end{cases} \tag{14}$$

$$\lambda = [12(1-\nu^2)]^{\frac{1}{4}}\, a/\sqrt{R_o h} \tag{15}$$

where ν is the Poisson's ratio.

In the case of ductile fracture one may need a fracture criterion which takes into account the ductile behavior of the material. Two such criteria based on the crack opening stretch and plastic instability were described in [5] and [1]. In either criteria the material's fracture resistance parameter may be expressed in the form of a "resistance pressure" which is a function of the crack length. For example, for steel cylinders the resistance pressure p_R or the load carrying capacity of the vessel may be expressed as [1]

$$p_R = p_Y[n + (1-n)e^{-\alpha\lambda}] \tag{16}$$

where n and α are constant ($0<n<1$, $\alpha>0$), λ is the shell parameter given by (15), and

$$p_Y = \frac{h\sigma_Y}{R_o} \ , \ \sigma_Y = \sigma_{YS}(1+\beta) \ , \ (0.05 < \beta < 0.15) \ . \tag{17}$$

Here σ_{YS} is the yield strength of the material, σ_Y is defined as the flow stress which is somewhat higher than σ_{YS}, and p_Y is the pressure corresponding to a "fully-yielded" cylinder. Thus, in this case the "crack driving force may be taken as either $p-p_R$ or $p^2-p_R^2$ and the following dynamic fracture

criteria may be expressed:

Model III:

$$\frac{d^2a}{dt^2} = \begin{cases} c_1(p-p_R) \ , \ \text{for } p > p_R \ , \\ c_1(p-p_R) - c_2(p-p_R)^2 \ , \ \text{for } p < p_R \ , \end{cases} \tag{18}$$

or Model IV:

$$\frac{d^2a}{dt^2} = \begin{cases} c_3(p^2-p_R^2) \ , \ \text{for } p > p_R \ , \\ c_3(p^2-p_R^2) - c_4(p^2-p_R^2)^2 \ , \ \text{for } p < p_R \ , \end{cases} \tag{19}$$

where again $c_1,..,c_4$ are constant. These as well as the constants $b_1,..,b_4$ have to be determined experimentally. Such experiments may be conducted on flat plates under ideal loading conditions and crack geometry.

The coupled depressurization and quasi-static crack propagation problem may now be solved by considering (9) and any one of the equations (11), (12), (18) or (19). The problem is a typical initial value problem which is highly nonlinear. It may be solved numerically by defining

$$\frac{da}{dt} = v(t) \tag{20}$$

and by observing that the differential equation (9) and the Models I to IV, i.e., (11), (12), (18) and (19) are of the form

$$\frac{dp}{dt} = f(a,p) \ , \tag{21}$$

$$\frac{d^2a}{dt^2} = \frac{dv}{dt} = g_i(a,p) \ , \quad (i=1,..,4) \ . \tag{22}$$

Using the initial conditions

$$a(0) = a_o \ , \quad v(0) = 0 \ , \quad p(0) = p_o \tag{23}$$

one may then write

$$p(t) = p_o + \int_o^t f(a,p)dt \ , \tag{24}$$

$$a(t) = a_o + \int_o^t v(t)dt \ , \tag{25}$$

$$v(t) = \int_o^t g_i(a,p)dt \ , \quad (i=1,..,4) \ . \tag{26}$$

and use any one of the integration formulas to obtain the unknown functions p, a, and v. The numerical calculations are terminated when either

$$v(t_A) = 0 \quad , \quad a(t_A) < 0.8\ell/2 \quad , \tag{27}$$

or

$$a(t_F) = 0.8\ell/2 \quad , \quad v(t_F) > 0 \quad . \tag{28}$$

where ℓ is the total length of the cylindrical container. The former situation corresponds to fracture arrest t_A being the arrest time and the latter basically implies catastrophic failure. The approximate limit $a = 0.8\ell/2$ is imposed by the shell analysis which is adopted from the infinitely long cylinder solution.

4. EXAMPLES AND DISCUSSION

As an example for a pressure tank with brittle or quasi-brittle fracture behavior a 20 in. diameter aluminum cylinder and for a pressure tank with ductile fracture behavior a 36 in. diameter steel cylinder is considered. In both cases the gas is assumed to be a biatomic ideal gas. The relevant information regarding the numerical data used in the calculations is given in Table I. The initial value problem as formulated by equations (9) and (10) or (20) to (23) was solved by using two sets of values for the crack propagation constants b_i, c_i, (i=1,..4) and d_1 (i.e., N=1 in (10)), which are shown in Table II. Other variables in the solution were the length of the cylinder ℓ, the discharge coefficient C_D, and the amount of the initial overload such as $k(0)-k_c$ or $p_o-p_R(0)$. Some of the typical results are shown in Figures 2 to 15.

Figures 2 to 5 show the results for the aluminum cylinder which was assumed to behave in a quasi-brittle manner. Here the length was varied between 20 in. and 200 in., the discharge coefficient was $0.5 \leq C_D \leq 0.8$, and the initial pressure overload was such that $50 \leq k(0)-k_c \leq 500$ psi$\sqrt{\text{in.}}$. Models I and II were used to calculate a(t), p(t), v(t), and k(t) using the constants shown in Table II. Figures 2 and 3 show the results obtained from Model I, i.e., equation (11), by using the constants given in columns A and B of Table II, respectively. In these as well as in the subsequent figures the computed values p, a, v, k, and p_R are normalized with respect

Table I. Data used in the examples

	Aluminum (Models I, II)		Steel (Models III, IV)	
a_o	0.5 in.	0.0127 m	1.9 in.	0.04826 m
h	0.1 in.	0.00254 m	0.403 in.	0.01024 m
R_o	10 in.	0.254 m	18 in.	0.4572 m
ℓ	200 in.	5.08 m	$\begin{cases} 50 \text{ in.} \\ 500 \text{ in.} \end{cases}$	$\begin{cases} 1.27 \text{ m} \\ 12.70 \text{ m} \end{cases}$
E	10^7 psi	$6.895 \times 10^{10} N/m^2$	3×10^7 psi	$20.685 \times 10^{10} N/m^2$
ν	0.3		0.3	
σ_{YS}	70 ksi	$48.265 \times 10^7 N/m^2$	65 ksi	$44.8175 \times 10^7 N/m^2$
σ_Y			75 ksi	$51.7125 \times 10^7 N/m^2$
k(0)	45.05 ksi$\sqrt{in}$	$4.945 \times 10^7 Nm^{-3/2}$		
k_c	45 ksi$\sqrt{in}$	$6.94 \times 10^7 Nm^{-3/2}$		
p_o	[illegible].65 psi	$2.1 \times 10^6 N/m^2$	1108.53 psi	$7643.314 \times 10^3 N/m^2$
$p_R(0)$			p_o-10 psi	$7574.364 \times 10^3 N/m^2$
R	238.752		238.752	
T_o	500°R	278°K	525°R	292°K
γ	1.4		1.4	
C_D	$\begin{cases} 0.5 \\ 0.8 \end{cases}$		$\begin{cases} 0.5 \\ 0.8 \end{cases}$	

Table II. Crack propagation constants (in units of lb, in, sec)

Model		A	B
I Eq. (11)	b_1	8×10^{-5}	8×10^{-4}
	b_2	4×10^{-7}	4×10^{-6}
II Eq. (12)	b_3	8×10^{-10}	8×10^{-9}
	b_4	4×10^{-17}	4×10^{-16}
III Eq. (18)	c_1	0.002	0.02
	c_2	0.001	0.01
IV Eq. (19)	c_3	$0.4/(p_o^2-p_R^2(0))$	$4/(p_o^2-p_R^2(0))$
	c_4	$80/(p_o^2-p_R^2(0))$	$800/(p_o^2-p_R^2(0))$
Eq. (10)	d_1	10^{-8}	10^{-7}

to a set of constants p_n, a_n, v_n, k_n, and p_{Rn} which are different for each example and are given by the figure captions. Thus the quantities shown in the figures are defined by

$$\bar{a} = a(t)/a_n \quad , \quad \bar{p} = p(t)/p_n \quad , \quad \bar{v} = v(t)/v_n$$

$$\bar{k} = k(t)/k_n \quad , \quad \bar{p}_R = p_R(t)/p_{Rn} \quad . \tag{29}$$

From the crack arrest view point these figures correspond to the most favorable conditions, that is, they were calculated for longer length ($\ell = 200$ in.), greater discharge coefficient ($C_D = 0.8$), and smaller overload ($k(0)-k_c = 50$ psi $\sqrt{\text{in}}$). Even in this case, in spite of the sharp decrease in the pressure and the stress intensity factor after a certain time, at $a = 0.8\ \ell/2$ the crack velocity v was still increasing. The basic conclusion here is that in gas-filled cylinders behaving in quasi-brittle manner it is unrealistic to expect any crack arrest.

Figures 4 and 5 show the results obtained from Model II, i.e., equation (11), by using the crack propagation constants given in columns A and B of Table II. Note th qualitatively these results are quite similar to those obtained from Model I.

The results for the steel cylinders are shown in Figures 6-13. Figures 6-9 show the results obtained from Model III, i.e., equation (18) for various combinations of ℓ, C_D, and c_1 and c_2 (see columns A and B in Table II). Here the figures show the driving pressure p and the resistance pressure p_R with the same scale. It is seen that for the short cylinder ($\ell = 50$ in) before the pressure drops below p_R, i.e., before the crack starts to decelerate, the crack length reaches 80 percent of the cylinder length, hence no crack arrest appears possible (Figures 6,7). On the other hand, in the long cylinder ($\ell = 500$ in) the crack is arrested before the crack length reaches $\ell/2$. Changing various constants in the calculations indicated that in the ductile fracture model, from the crack arrest view point the most important variable was the cylinder length. For example, comparing Figures 8 and 9 it may be seen that in spite of one order of magnitude difference in crack propagation constants c_1, c_2 (see columns A and B in Table II), the results are qualitatively the same. Higher values of c_1 and c_2 simply shortens the crack arrest time. In the results shown in Figures 8, 9, 12, and 13 where crack arrest took place, the calculations were stopped when the crack velocity dropped to zero.

The results obtained form Model IV (equation (19)) are shown in Figures 10-13. Except for the shortened time scale, these results are quite similar to those obtained from Model III.

The results obtained from the velocity model (10) with $N = 1$ are shown in Figures 14 and 15. In these calculations too the influence of crack velocity on k_c or G_c is neglected. The highest velocity observed here is approximately one-fourth of the shear wave velocity of the material, meaning that the inertia effects may still not be all that crucial. It is seen that qualitatively these results are quite similar to those obtained by using the acceleration Models I and II, the important difference being in the time scale. In both cases there does not seem to be sufficient time for any

significant depressurization. Hence, the problem is analogous to the centrally cracked flat plate problem under constant tensile stress with the additional magnification in the "crack driving force" k^2 coming from the shell curvature effect.

The sample calculations given in this paper indicate that in order to deal with the crack propagation and arrest phenomenon the fracture criterion must be cast in dynamic form relating the time rates of the crack length to the overload. Developing such dynamic fracture criteria does not seem to be a major problem. The main difficulty in this respect lies in determining the related crack propagation constants. This may be done by conducting carefully designed experiments in which the crack length and the appropriate load factor are accurately measured or calculated and the corresponding resistance parameter is independ ntly estimated. The preliminary calculations given in this paper also indicate that in most finite volume containers it is very likely that the crack velocity will always be sufficiently low to justify the quasi-static assumption in the shell analysis.

REFERENCES

1. Erdogan, F., Irwin, G. R. and Ratwani, M., "Ductile Fracture of Cylindrical Vessels Containing a Large Flaw", *9th National Symposium on Fracture Mechanics*, to be published by ASTM.

2. *Fatigue Crack Propagation*, ASTM STP 415, 1967.

3. Johnson, H. H. and Paris, P. C., "Subcritical Flaw Growth", *Engineering Fracture Mechanics*, Vol. 1, 1968, p. 3.

4. *The Surface Crack*, J. Swedlow, Ed., American Society of Mechanical Engineers, New York, 1972.

5. Erdogan, F. and Ratwani, M., "Fracture Initiation and Propagation in a Cylindrical Shell Containing an Initial Surface Flaw", *Nuclear Engineering and Design*, Vol. 27, 1974, p. 14.

6. Paris, P. C. and Erdogan, F., "A Critical Analysis of Crack Propagation Laws", *J. Basic Engineering, Trans. ASME*, Series D, Vol. 85, 1963, p. 528.

7. Erdogan, F. and Ratwani, M., "Fatigue and Fracture of Cylindrical Shells Containing a Circumferential Crack", *Int. J. Fracture Mechanics*, Vol. 6, 1970, p. 379.

8. Newman, J. C., Jr., "Fracture Analysis of Surface and Through Cracked Sheets and Plates", *Engineering Fracture Mechanics*, Vol. 5, 1973, p. 667.

9. Landes, J. D. and Begley, J. A., "The Effect of Specimen Geometry on J_{IC}", ASTM-STP 514, 1972, p. 24.

10. Erdogan, F., "Crack Propagation Theories", *Fracture*, H. Liebowitz, Ed., Vol. II, 1968, Academic Press, Inc., New York.

11. Erdogan, F., and Ratwani, M., "Plasticity and Crack Opening Displacement in Shells", *Int. J. Fracture Mechanics*, Vol. 8, 1972, p. 413.

12. Erdogan, F. and Kibler, J. J., "Cylindrical and Spherical Shells with Cracks", *Int. J. Fracture Mechanics*, Vol. 5, 1969, p. 229.

13. Erdogan, F. and Ratwani, M., "Fracture of Cylindrical and Spherical Shells Containing a Crack", *Nuclear Engineering and Design*, Vol. 20, 1972, p. 265.

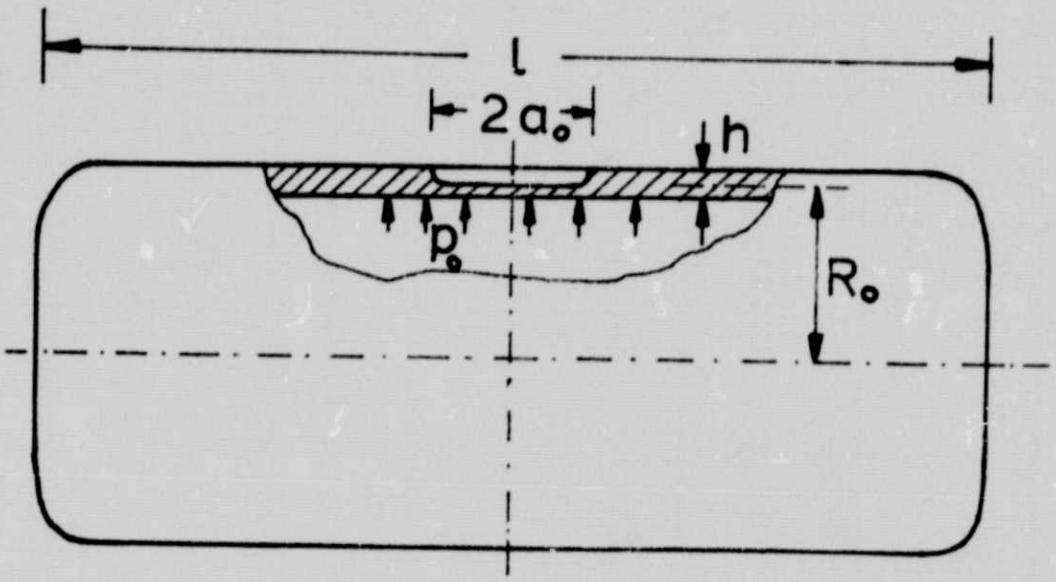

Figure 1. Geometry of the pressurized cylindrical container.

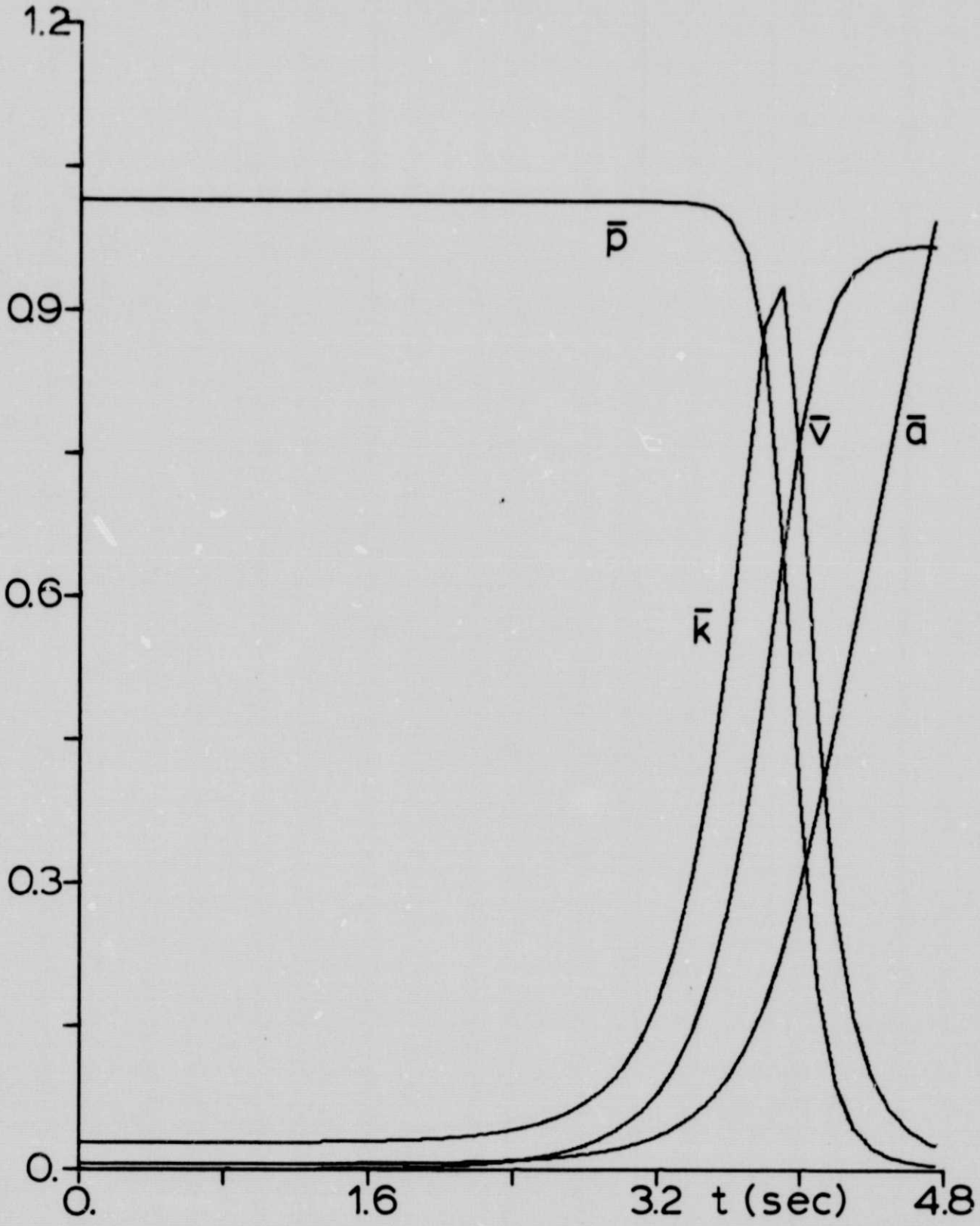

Figure 2. Results for the 20 in. diameter aluminum vessel; $\ell = 200$ in., $C_D = 0.8$, Model I with constants in column A, Table II. The normalization constants: $p_n = 300$ psi, $a_n = 80$ in., $v_n = 80$ in/sec., $k_n = 16 \times 10^5$ psi $\sqrt{\text{in.}}$

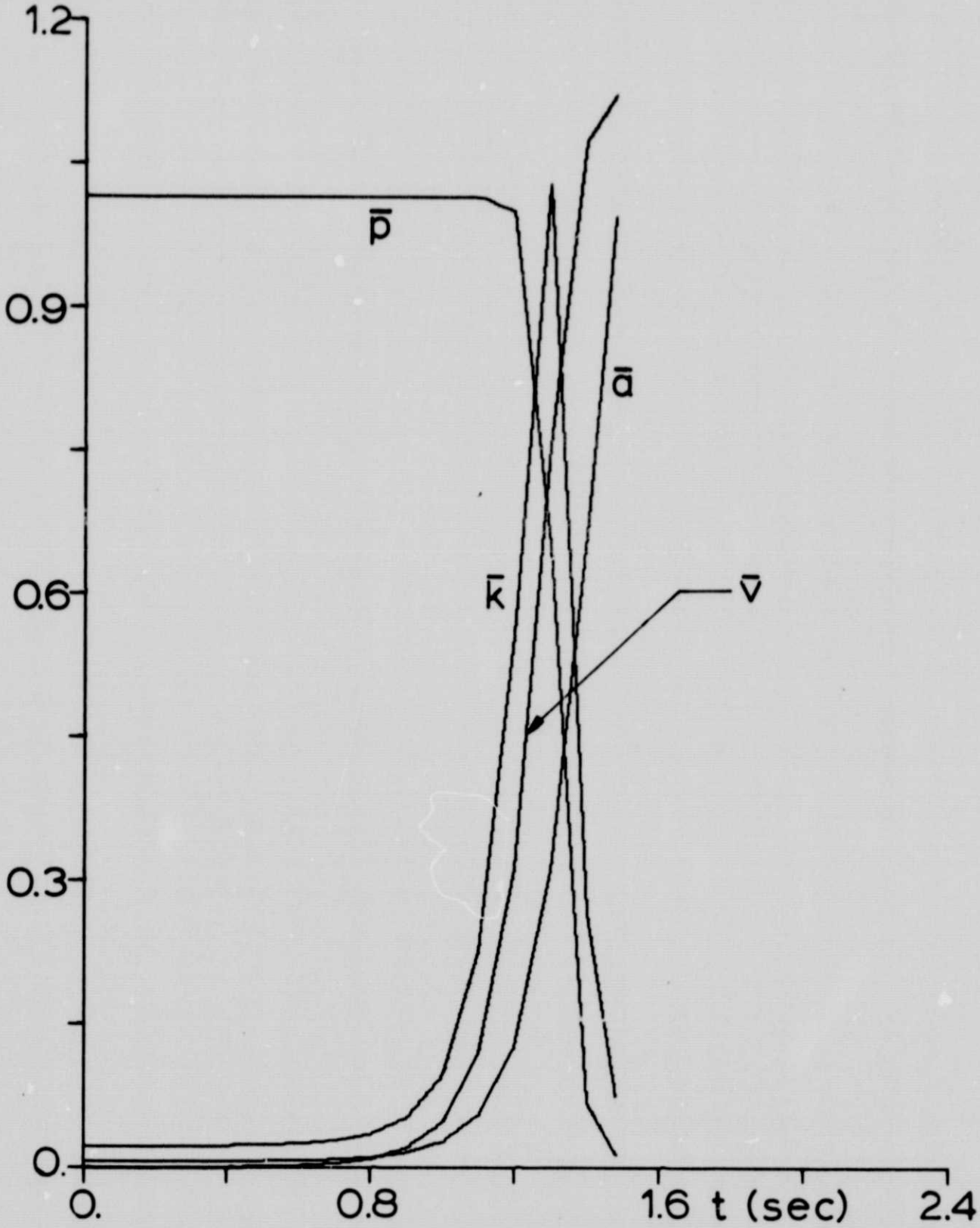

Figure 3. Results for the 20 in. diameter aluminum vessel; $\ell = 200$ in., $C_D = 0.8$, Model I with constants in column B, Table II. The normalization constants: $p_n = 300$ psi, $a_n = 80$ in., $v_n = 300$ in/sec. $k_n = 2 \times 10^6$ psi $\sqrt{\text{in.}}$

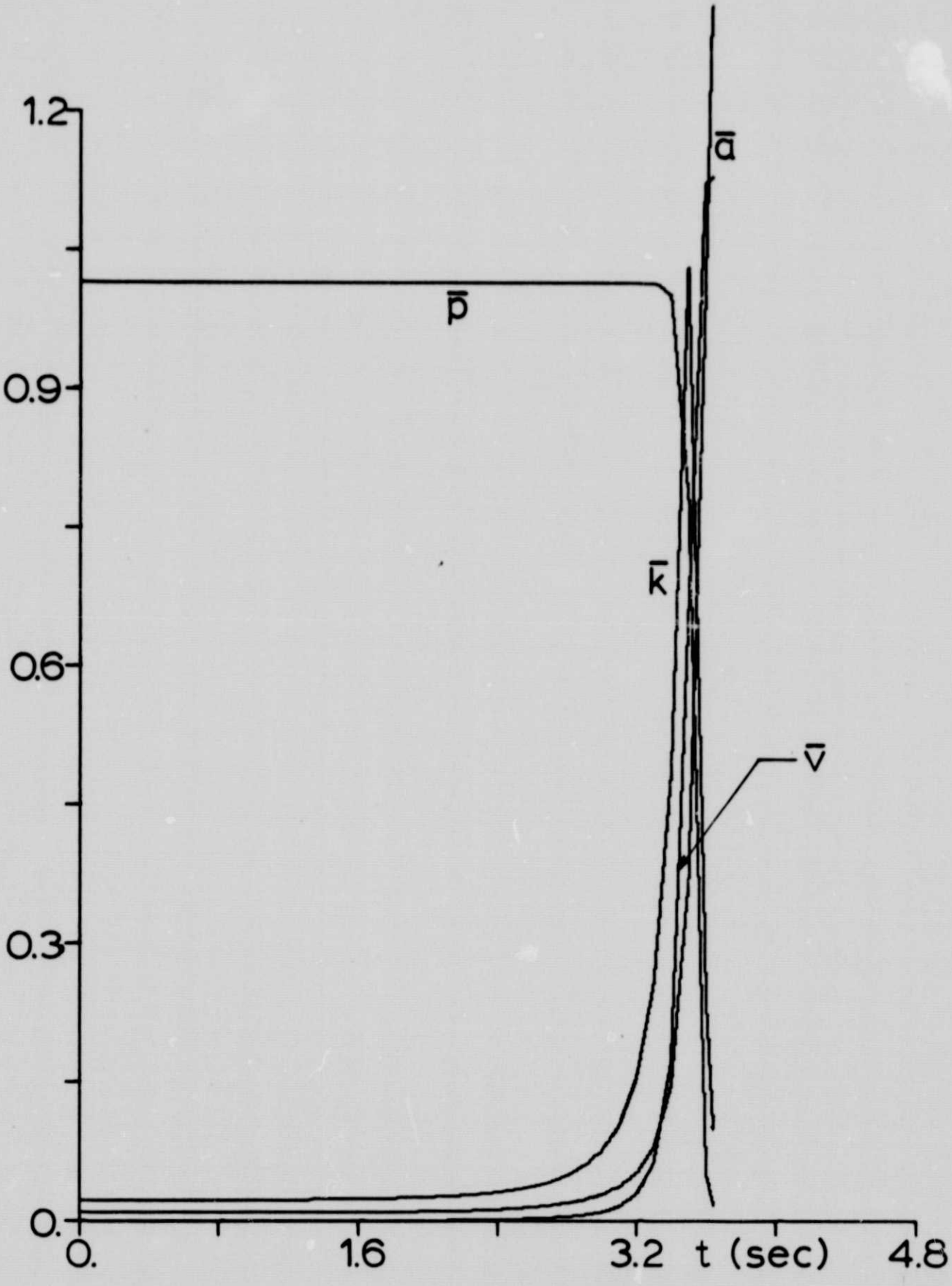

Figure 4. Results for the 20 in. diameter aluminum vessel; $\ell = 200$ in., $C_D = 0.8$, Model II with constants in column A, Table II. The normalization constants: $p_n = 300$ psi, $a_n = 60$ in., $v_n = 400$ in/sec., $k_n = 20 \times 10^5$ psi $\sqrt{\text{in.}}$

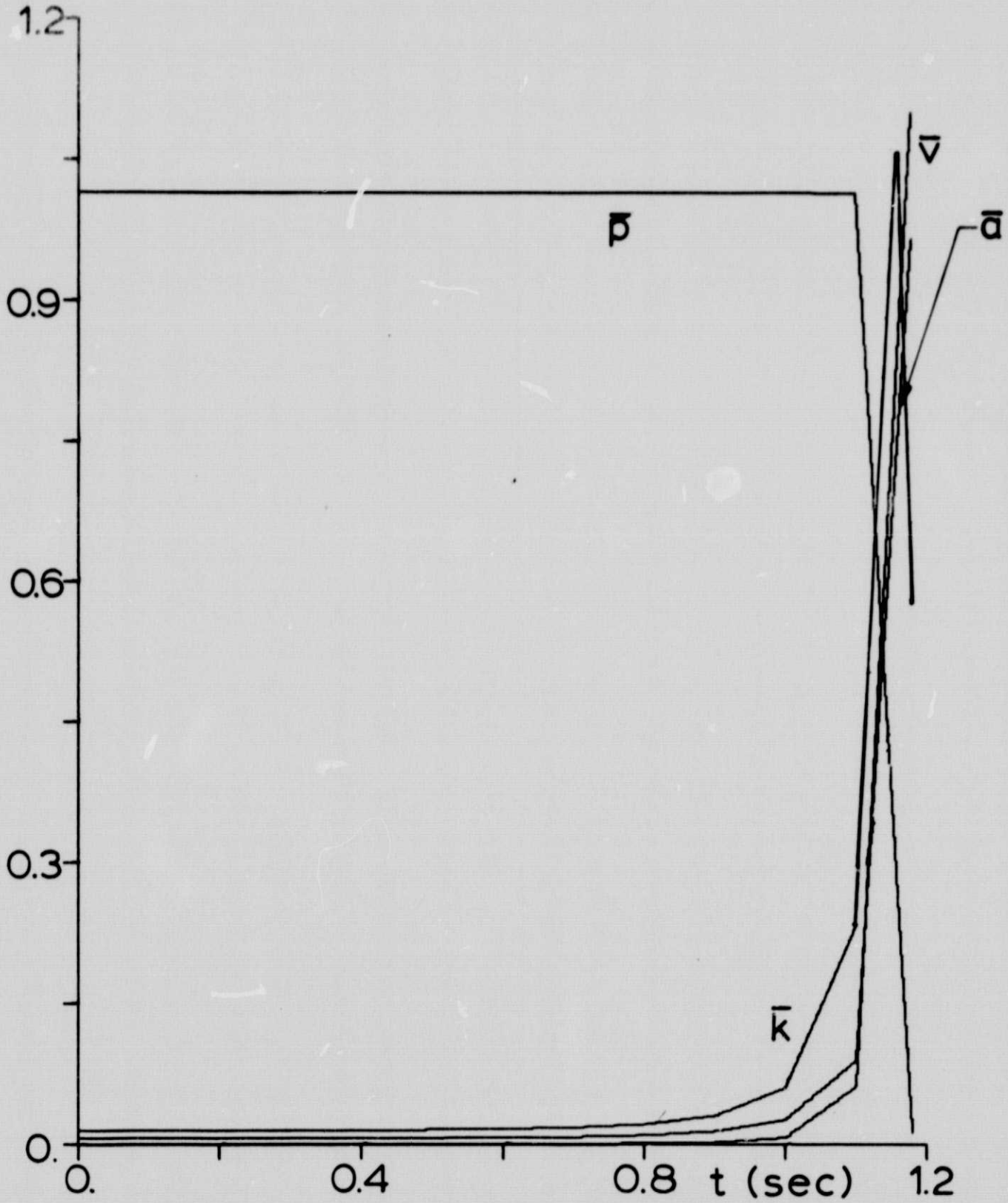

Figure 5. Results for the 20 in. diameter aluminum vessel; $\ell = 200$ in., $C_D = 0.8$, Model II with constants in column B, Table II. The normalization constants: $p_n = 300$ psi, $a_n = 80$ in., $v_n = 2500$ in/sec., $k_n = 3 \times 10^6$ psi $\sqrt{\text{in.}}$

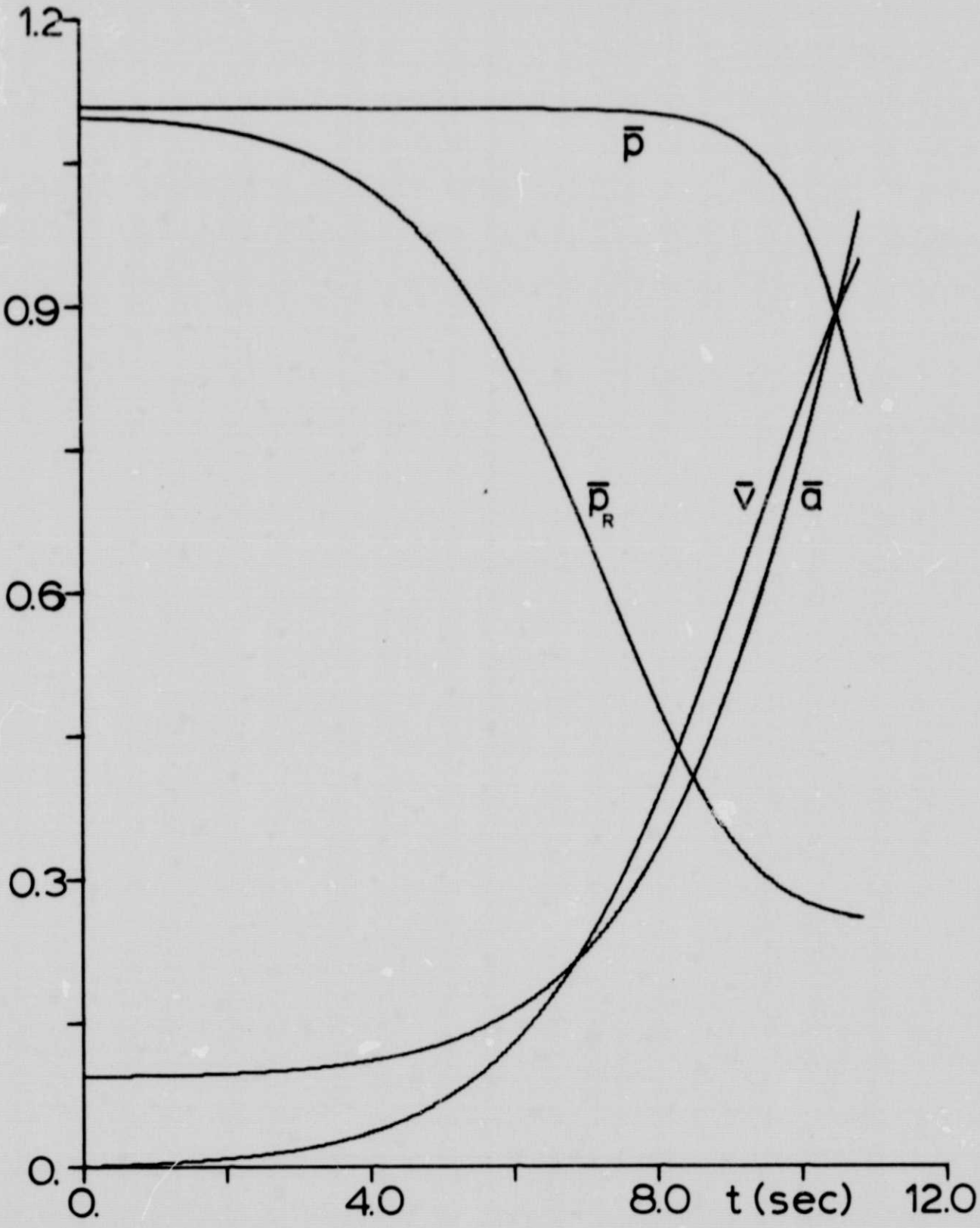

Figure 6. Results for the 36 in. diameter steel vessel; $\ell = 50$ in., $C_D = 0.5$, Model III with constants in column A, Table II. The normalization factors: $p_n = 1000$ psi, $a_n = 20$ in., $v_n = 7$ in/sec. $p_{Rn} = 1000$ psi.

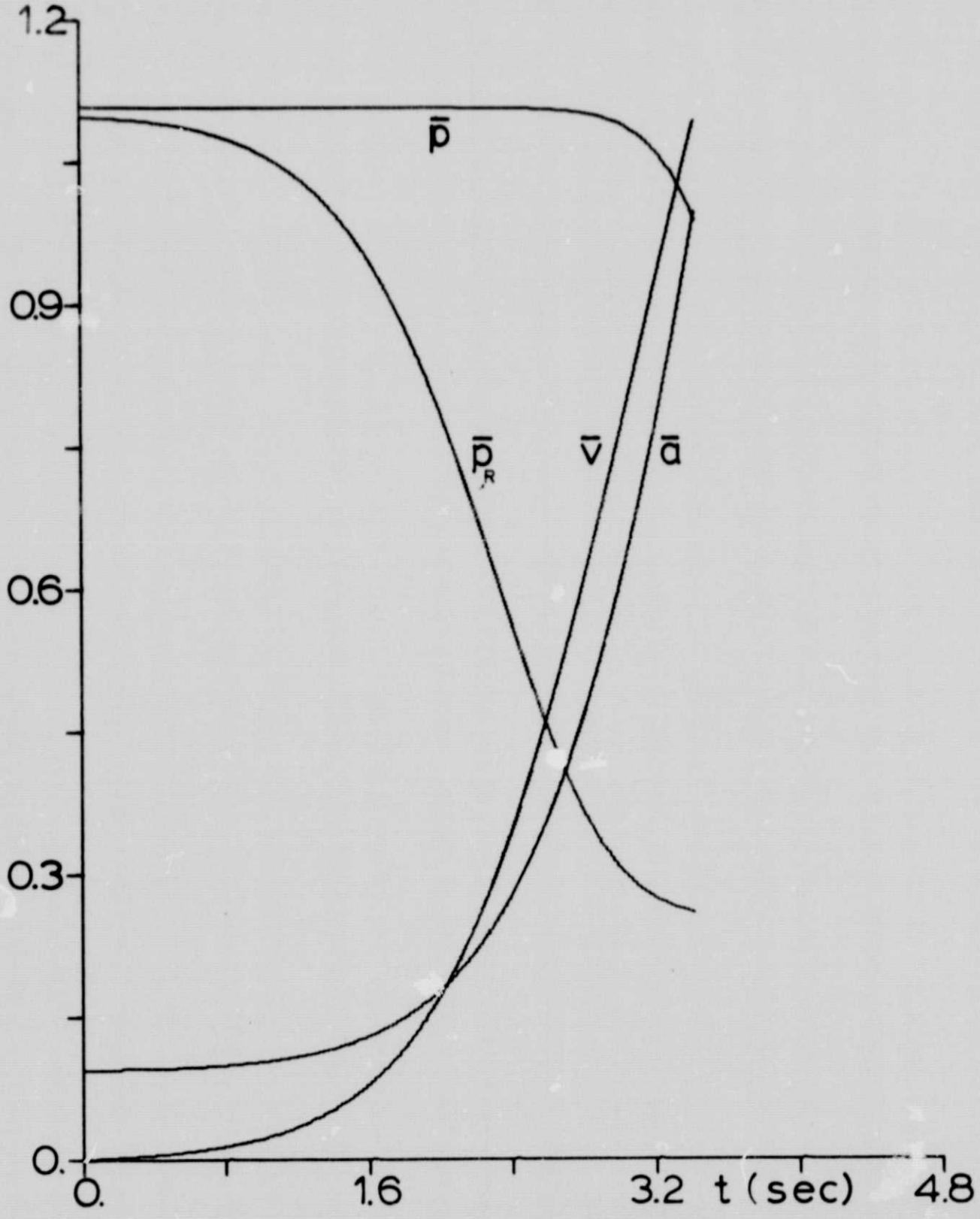

Figure 7. Results for the 36 in. diameter steel vessel; $\ell = 50$ in., $C_D = 0.5$, Model III with constants in column B, Table II. The normalization factors: $p_n = p_{Rn} = 1000$ psi, $a_n = 20$ in., $v_n = 20$ in/sec.

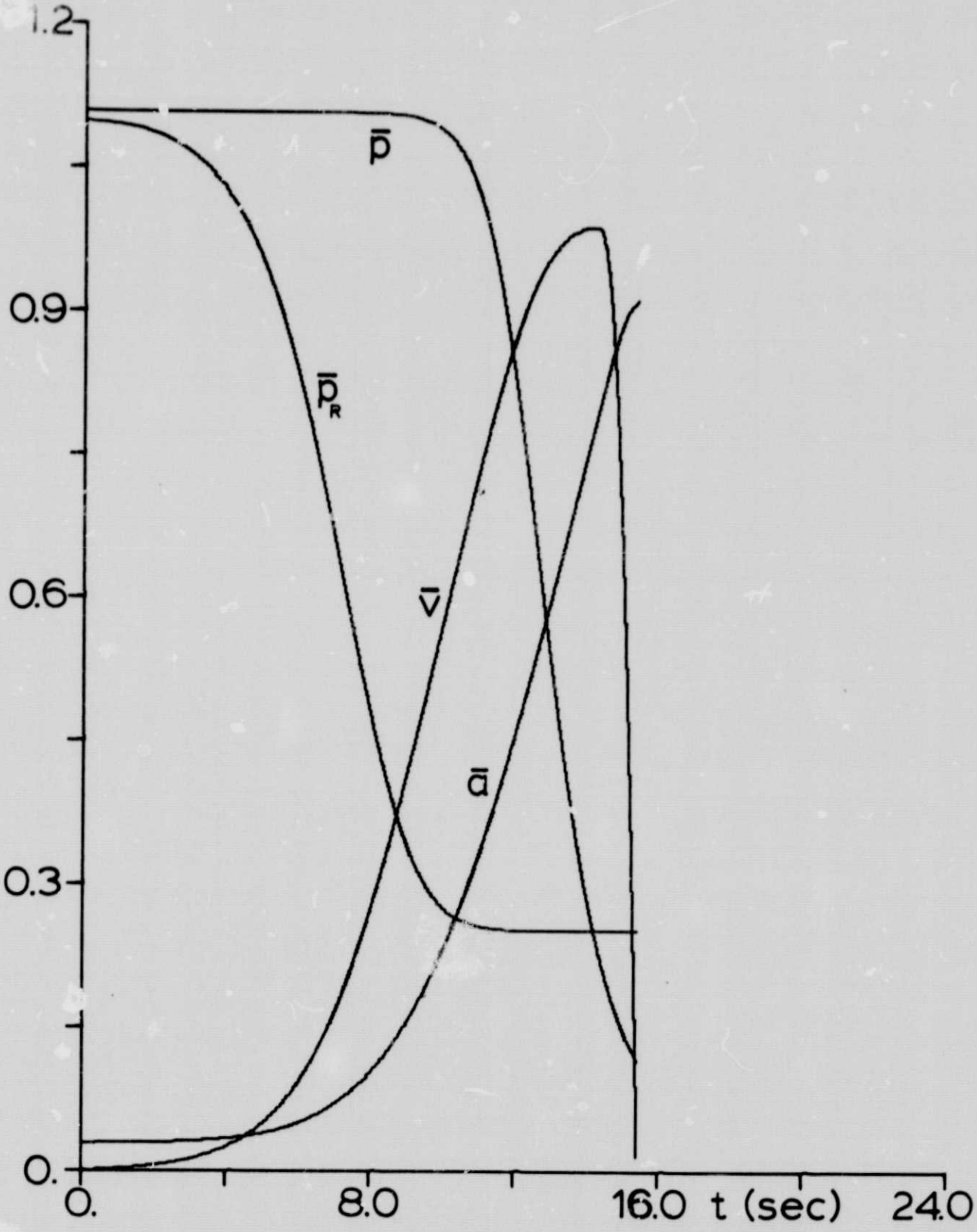

Figure 8. Results for the 36 in. diameter steel vessel; $\ell = 500$ in., $C_D = 0.8$, Model III with constants in column A, Table II. Normalization factors: $p_n = p_{Rn} = 1000$ psi, $a_n = 65$ in., $v_n = 10$ in/sec.

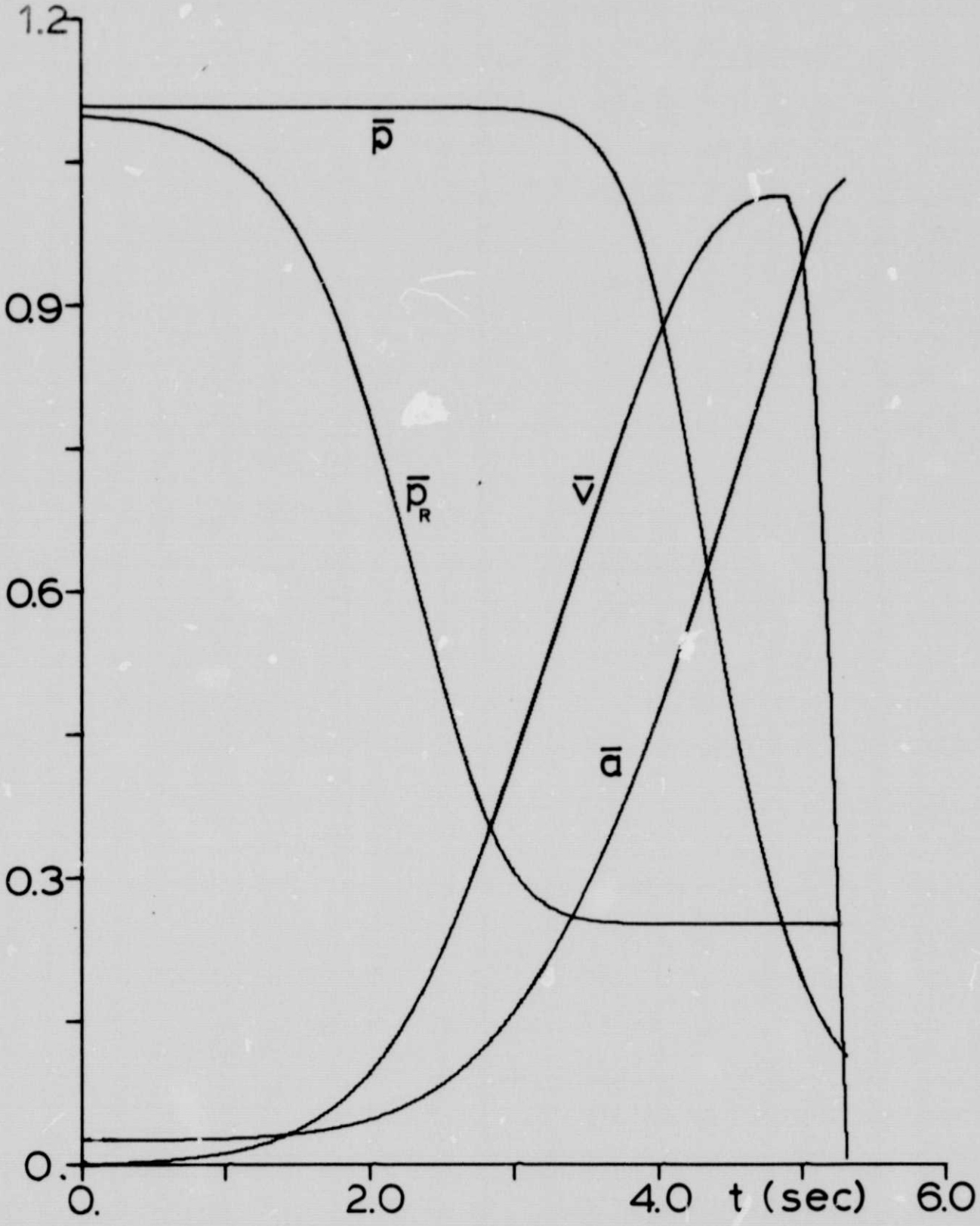

Figure 9. Results for the 36 in. diameter steel vessel: $\ell = 500$ in., $C_D = 0.8$, Model III with constants in column B, Table II. Normalization factors: $p_n = p_{Rn} = 1000$ psi, $a_n = 75$ in., $v_n = 36$ in/sec.

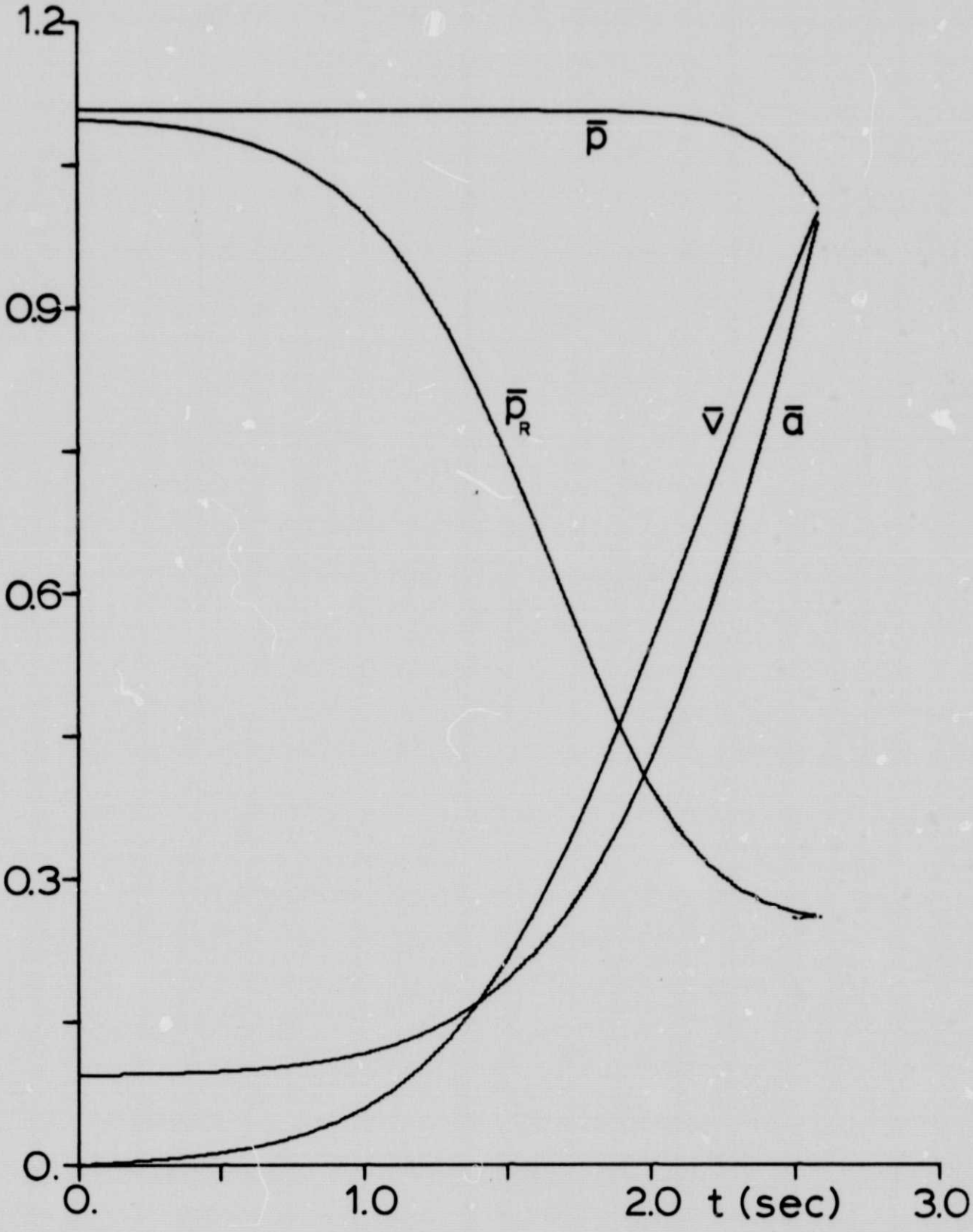

Figure 10. Results for the 36 in. diameter steel vessel; $\ell = 50$ in., $C_D = 0.5$, Model IV with constants in column A, Table II. The normalization factors: $p_n = p_{Rn} = 1000$ psi, $a_n = 20$ in., $v_n = 25$ in/sec.

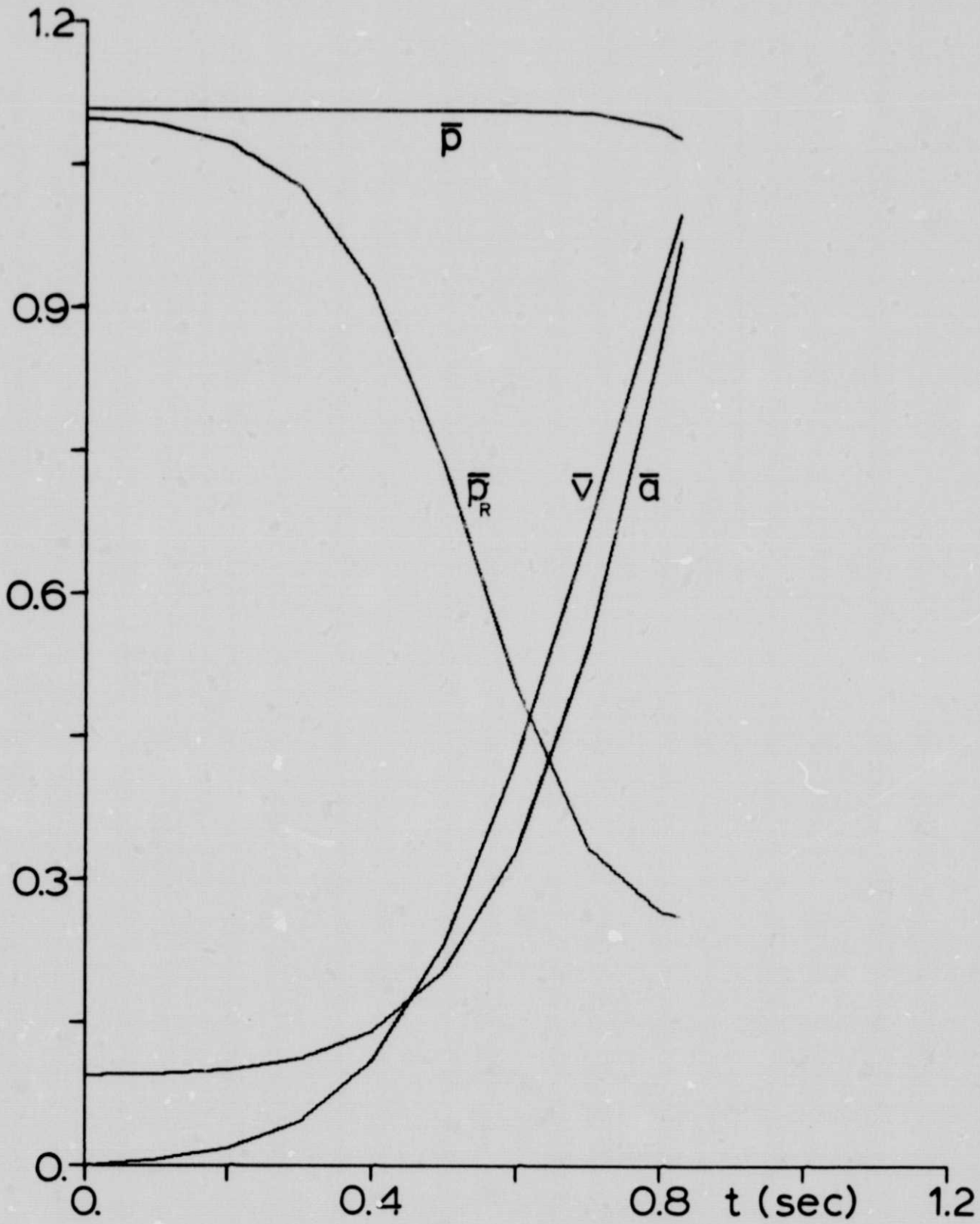

Figure 11. Results for the 36 in. diameter steel vessel; $\ell = 50$ in., $C_D = 0.5$, Model IV with constants in column B, Table II. The normalization factors: $p_n = p_{Rn} = 1000$ psi, $a_n = 20$ in., $v_n = 80$ in/sec.

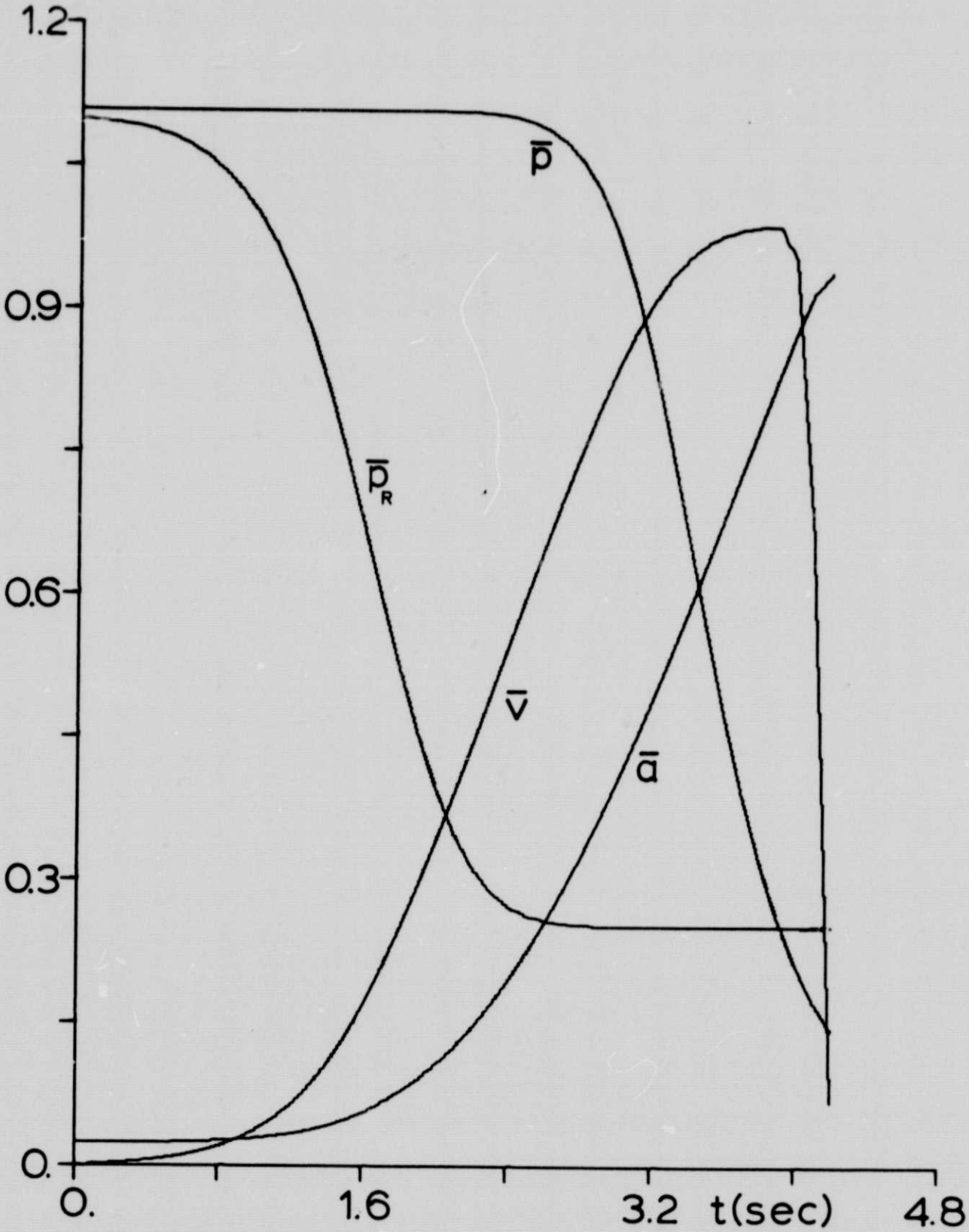

Figure 12. Results for the 36 in. diameter steel vessel; $\ell = 500$ in., $C_D = 0.8$, Model IV with constants in column A, Table II. The normalization factors: $p_n = p_{Rn} = 1000$ psi, $a_n = 30$ in., $v_n = 40$ in/sec.

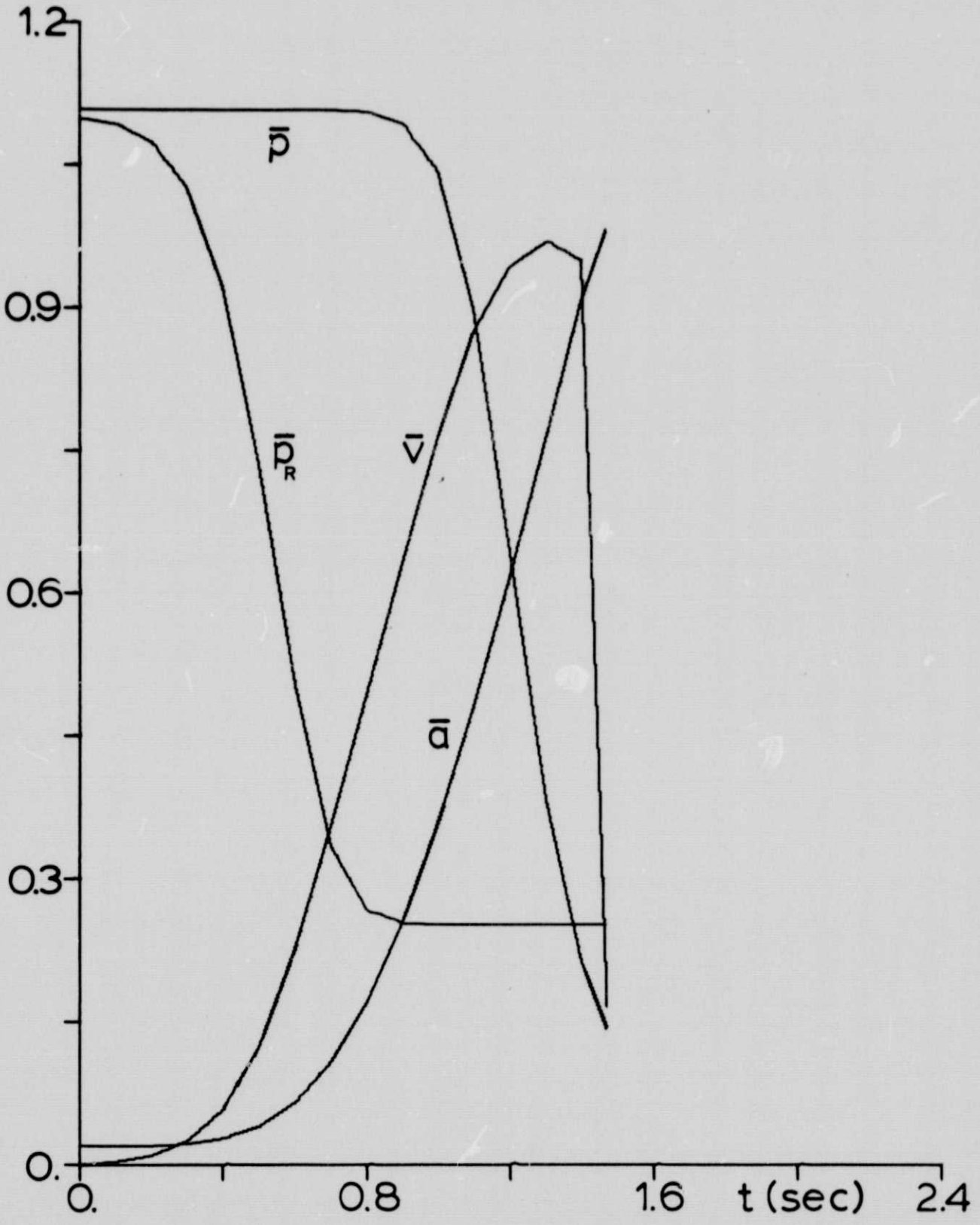

Figure 13. Results for the 36 in. diameter steel vessel; $\ell = 500$ in., $C_D = 0.8$, Model IV with constants in column B, Table II. The normalization factors: $p_n = p_{Rn} = 1000$ psi, $a_n = 100$ in., $v_n = 150$ in/sec.

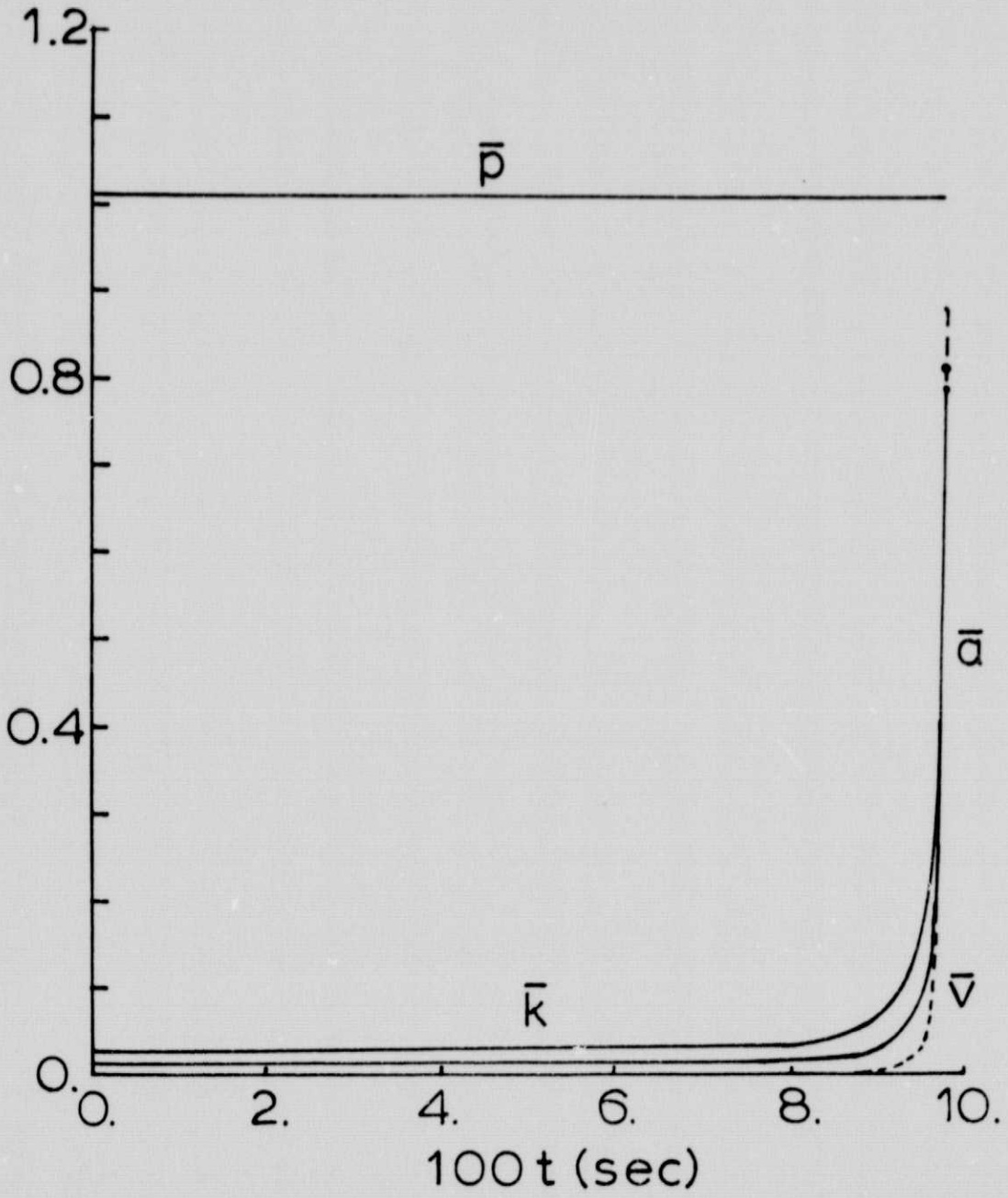

Figure 14. Results for the 20 in. diameter aluminum cylinder; $\ell = 200$ in., $C_D = 0.8$. The velocity model, Eq. (10), $d_1 = 10^{-8}$; normalization factors: $a_n = 50$ in., $p_n = 300$ psi., $v_n = 30{,}000$ in/sec., $k_n = 2 \times 10^6$ psi $\sqrt{\text{in.}}$

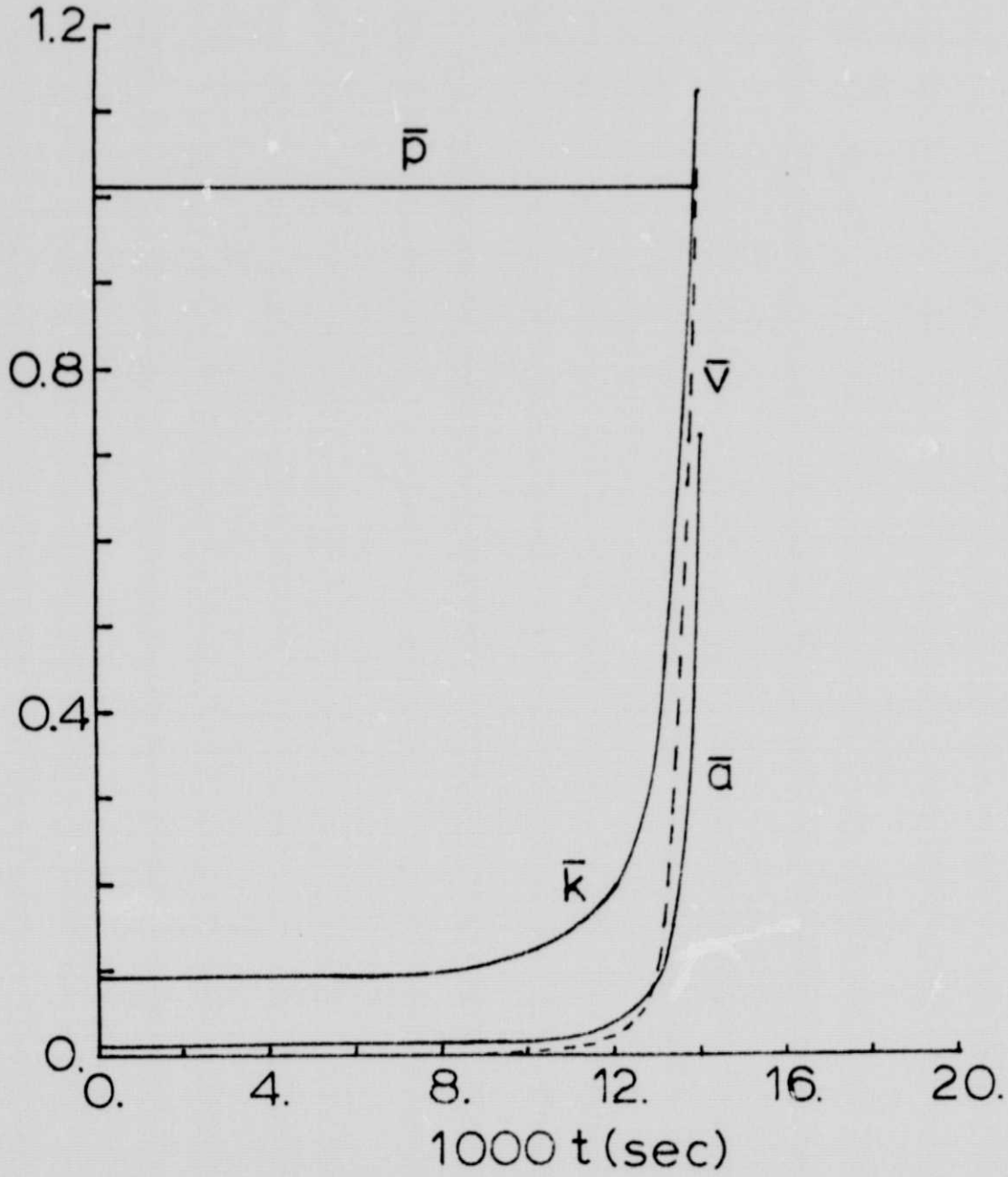

Figure 15. Results for the 20 in. diameter aluminum cylinder; $\ell = 200$ in., $C_D = 0.8$. The velocity model, Eq. (10), $d_1 = 10^{-7}$; normalization factors: $a_n = 50$ in., $p_n = 300$ psi., $v_n = 30{,}000$ in/sec., $k_n = 5 \times 10^5$ psi $\sqrt{\text{in.}}$